# Hypoxia induces the dormant state in oocytes through expression of Foxo3

島本, 走

https://doi.org/10.15017/2534393

出版情報：Kyushu University, 2019, 博士（医学）, 課程博士
バージョン：
権利関係：

# Hypoxia induces the dormant state in oocytes through expression of *Foxo3*

So Shimamoto[a], Yohei Nishimura[a], Go Nagamatsu[a], Norio Hamada[a], Haruka Kita[a], Orie Hikabe[a], Nobuhiko Hamazaki[a], and Katsuhiko Hayashi[a,1]

[a]Department of Stem Cell Biology and Medicine, Graduate School of Medical Sciences, Kyushu University, Fukuoka 812 8582, Japan

Edited by Janet Rossant, Hospital for Sick Children, University of Toronto, Toronto, Canada, and approved May 9, 2019 (received for review October 9, 2018)

**In mammals, most immature oocytes remain dormant in the primordial follicles to ensure the longevity of female reproductive life. A precise understanding of mechanisms underlying the dormancy is important for reproductive biology and medicine. In this study, by comparing mouse oogenesis in vivo and in vitro, the latter of which bypasses the primordial follicle stage, we defined the gene-expression profile representing the dormant state of oocytes. Overexpression of constitutively active FOXO3 partially reproduced the dormant state in vitro. Based on further gene-expression analysis, we found that a hypoxic condition efficiently induced the dormant state in vitro. The effect of hypoxia was severely diminished by disruption of the *Foxo3* gene and inhibition of hypoxia-inducible factors. Our findings provide insights into the importance of environmental conditions and their effectors for establishing the dormant state.**

oocytes | hypoxia | *Foxo3*

The germ-cell lineage is crucial for perpetuating species, as it has an exclusive function to create new individuals. In the female germ line, primordial germ cells (PGCs) proliferate in the developing gonads as germ-cell cysts, in which the germ cells are connected to each other through intercellular bridges (1), and then enter meiosis at embryonic day (E) 13.5 (2). These germ-cell cysts are gradually fragmented at later embryonic stages, and, finally, follicle structures are formed by postnatal day (P) 3 (3). There are two types of follicles at this stage: One type of follicles immediately starts oocyte growth, and the other type is arrested as primordial follicles, in which a single dormant oocyte is surrounded by squamous granulosa cells (3). Several reports have described an oocyte-intrinsic regulatory mechanism for maintenance of the dormant state. *Foxo3* is known to play a key role in maintenance of the dormant state. *Foxo3*-disrupted mice quickly lose their fertility due to the overactivation of immature follicles (4). FOXO3 is regulated by the phosphorylation via a phosphatidylinositol-3 kinase (PI3K)-mediated signal. Upon phosphorylation, FOXO3 is transported from the nucleus to the cytoplasm, thus triggering oocyte growth. Disruption of *Pten*, a negative regulator of PI3K signaling, leads to an overactivation of follicles similar to that by *Foxo3* knockout (KO) (4, 5). Although these genetic analyses identified genes involved in the dormant state, the mechanisms establishing the dormant state are still elusive. This is partially due to the lack of a culture system that robustly reproduces the process occurring at the perinatal stage.

Recently, we developed a culture method in which functional oocytes can be induced from pluripotent stem cells (6, 7). In the in vitro differentiation (IVDi) culture system, pluripotent stem cells bearing *Blimp1–mVenus* (BV) and *Stella–ECFP* (SC) reporter transgenes (8) were first differentiated into PGC-like cells (PGCLCs). PGCLCs bearing BV and SC were aggregated with E12.5 gonadal somatic cells (9). After 3 wk of culture of the aggregates, hereinafter called reconstituted ovaries (rOvaries), primary oocytes in secondary follicles could be obtained. Although the gene expression of oocytes in the secondary follicles in vitro was comparable to that of oocytes in vivo, the process from PGCLCs to oocytes in vitro differed from that observed in vivo. That is, during IVDi culture, the oocytes were not arrested at the primordial follicle stage but began their maturation (Fig. 1*A*). Since primordial follicles are merely formed in IVDi, the culture system would be a useful tool for reconstituting the dormant state of oocytes in primordial follicles. In this study, therefore, we use the IVDi culture system to explore the mechanisms involved in establishing the dormant state of oocytes.

## Results

**No Primordial Follicles Were Formed in IVDi Culture.** During IVDi, the BV signal was gradually lost, while the SC signal was maintained throughout the 3-wk culture in rOvaries (Fig. 1*A*). Most follicles reached the secondary follicle stage at day (D) 21 of culture, while small oocytes were barely observed at this time point (*SI Appendix*, Fig. S1*A*). In contrast, the P6 ovary in vivo bearing the SC reporter showed a number of small oocytes in addition to growing oocytes (*SI Appendix*, Fig. S1*B*). Immunofluorescence (IF) analysis revealed that oocytes in the rOvaries had formed cyst-like structures by D5 and gradually fragmented from D7 to D9 (Fig. 1*B*). Follicle structures appeared in the rOvaries at around D11 and gradually grew into secondary follicles by D17 (Fig. 1*B* and *SI Appendix*, Fig. S1*C*). IF analysis using anti-FOXO3 antibody revealed that FOXO3 was detected in the cytoplasm of embryonic stem cell (ESC)-derived oocytes from D9 (Fig. 1*B* and *SI Appendix*, Fig. S1*C*). After the formation of follicle structures from D11, the FOXO3 protein remained localized in the cytoplasm throughout the development of oocytes (Fig. 1*B* and *SI Appendix*, Fig. S1*C*), which were similar in appearance to oocytes in activated follicles in vivo (*SI Appendix*, Fig. S1*D*). These were contrasted to primordial follicles in vivo, in which FOXO3 is localized in nuclei of the oocytes (*SI Appendix*, Fig. S1*D*). FOXO3 was localized at the cytoplasm in >91.3% of FOXO3-positive oocytes in vitro at D9–17 (Fig. 1*B*). Thus, these data demonstrated that oogenesis in vitro failed to establish the dormant state of oocytes.

### Significance

**This study using a unique culture system revealed that hypoxia induces the dormant state in oocytes through FOXO3. Hypoxia-inducible factors are involved in maintenance of the dormant oocytes under a hypoxic condition. These findings provide mechanistic insight into the transduction of environmental cues that regulate genes involved in the dormant state of oocytes.**

Author contributions: S.S. and K.H. designed research; S.S., Y.N., G.N., N. Hamada, H.K., O.H., and N. Hamazaki performed research; S.S. and K.H. analyzed data; S.S. and K.H. wrote the paper.

The authors declare no conflict of interest.

This article is a PNAS Direct Submission.



Data deposition: The data reported in this paper have been deposited in the Gene Expression Omnibus (GEO) database, https://www.ncbi.nlm.nih.gov/geo (accession no. GSE128305).

[1]To whom correspondence may be addressed. Email: hayashik@hgs.med.kyushu-u.ac.jp.

This article contains supporting information online at www.pnas.org/lookup/suppl/doi:10.1073/pnas.1817223116/-/DCSupplemental.

Published online May 30, 2019.

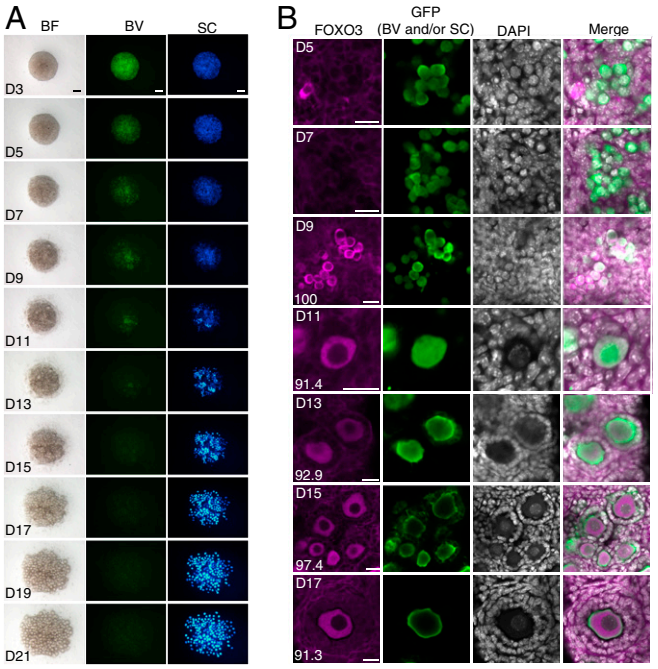


**Fig. 1.** Few dormant oocytes in IVDi culture. (*A*) Oocyte differentiation during IVDi. Representative images of an rOvary cultured for the number of days (D) indicated are shown. BF, bright field. (Scale bars, 200 μm.) (*B*) Localization of FOXO3 during IVDi. IF images of FOXO3, GFP (BV and/or SC), and DAPI are shown. The numbers at the upper left and the lower left indicate the day of culture and the percentage of oocytes with cytoplasmic FOXO3, respectively. The numbers of samples examined were 67 (D9), 58 (D11), 56 (D13), 38 (D15), and 46 (D17). (Scale bars, 20 μm.)

**Global Transcription Dynamics along Oocyte Development In Vivo and In Vitro.** To gain insights into the molecular mechanisms responsible for the difference between oogenesis in vivo and in vitro, we performed a transcriptome analysis [RNA sequencing (RNA-seq)]. SC-positive oocytes were isolated from ovaries of E14.5, E16.5, and E18.5 embryos and of P1, P3, P4, and P6 pups and rOvaries at D5, D7, D9, D10, D11, D13, D15, D17, and D20 (*SI Appendix*, Fig. S2 *A* and *B*). For P4 and P6 oocytes, we separated oocytes in accordance with their size (*SI Appendix*, Fig. S2 *A–C*). Principal component analysis (PCA) revealed that oocytes in vivo changed their transcriptomes as they developed from E14.5 to P1 (Fig. 2*A*). In contrast, the transcriptomes were similar among P3, P4 small, and P6 small oocytes in vivo (Fig. 2*A*), indicating that the dormant state was maintained in these oocyte fractions. The transcriptomes of P4 large and P6 large oocytes were quite distinct from those of the dormant population (Fig. 2*A*), suggesting that a drastic change of transcriptomes occurred upon follicular activation. PCA of oocytes in vitro revealed that oocytes from D5 to D9 developed in a similar manner to those in vivo from E14.5 to E16.5. However, it also showed that oocytes in vitro after D11 showed a slightly different pathway from oocytes in vivo. The difference became more prominent after D13: Transcriptomes of D13 oocytes were clearly different from those of the oocytes in the dormant state in vivo, and those of oocytes at D15 and D17 were rather similar to those of P4 large and P6 large oocytes in vivo (Fig. 2*A*). These results suggested that oocytes in vitro were directly activated without first entering the dormant state.

A heatmap of correlation coefficients between transcriptomes of oocytes at different developmental stages indicated that oocytes in vivo are clustered into three groups (Fig. 2*B*): (*i*) embryonic oocytes (E14.5, E16.5, and E18.5); (*ii*) dormant oocytes (P1, P3, P4 small, and P6 small); and (*iii*) growing oocytes (P4 large and P6 large). Oocytes in vitro from D7 to D11 were clustered tightly with embryonic oocytes, whereas those after D13 were clustered with a group of growing oocytes (Fig. 2*B*). These data reinforced the notion that oocytes in the rOvaries were directly activated after follicle formation. To clarify the transition from embryonic oocytes to the dormant state, we investigated transcriptomic change from E16.5 to P3. There were a number of differentially expressed genes (DEGs) gradually decreased along with oocyte development toward P3 dormant oocytes (*SI Appendix*, Fig. S3*A*). Gene Ontology (GO) analysis showed that genes up-regulated during this process were enriched with genes related

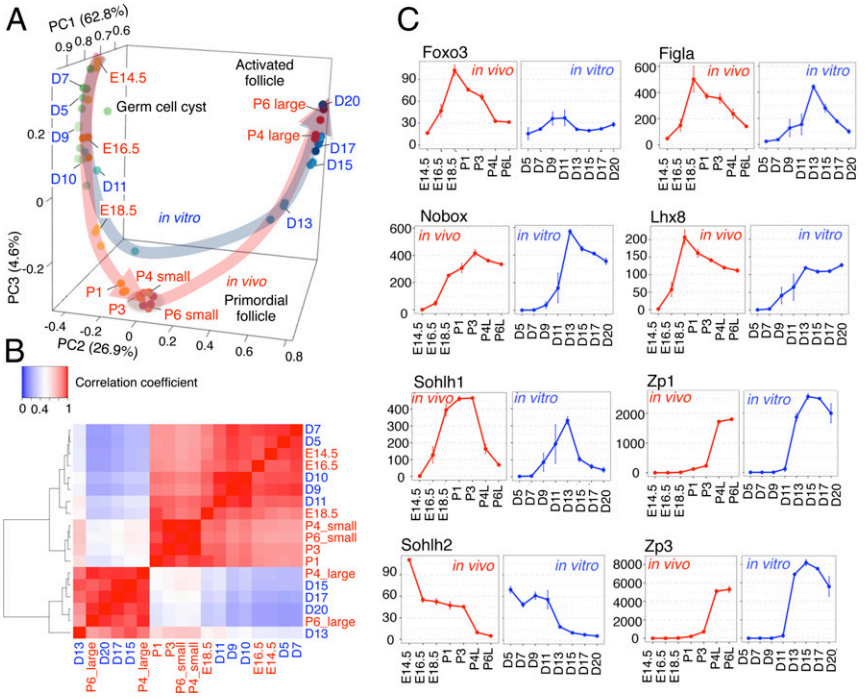


**Fig. 2.** Distinct gene-expression profiles during oogenesis in vivo and in vitro. (*A*) Gene-expression dynamics during oogenesis in vivo and in vitro. PCA of oocytes at each developmental stage indicated is shown. D, days of culture in IVDi. (*B*) Heatmap analysis of gene-expression profiles of oocytes in vivo and in vitro. Pearson correlation coefficients among oocytes at the indicated stages are shown. The heatmap and clustering are based on the average reads per kilobase million (RPKM) gene expression levels. (*C*) Gene-expression dynamics of genes necessary for oogenesis. The averaged RPKM values of each of the indicated genes are shown. Bars at each point indicate the SD based on three independent experiments.

to oxidative stress processes, such as the "response to oxidative stress" and the "oxidation-reduction process," indicating that mechanisms dealing with oxidative stress were active during this developmental period (*SI Appendix*, Fig. S3*B*). Oxidative stress is commonly known as a major factor involved in cell damage and aging. It is possible that the dormant state is involved in regulating the quality of the oocytes to ensure the upcoming oocyte growth. Genes down-regulated during the transition were related to meiosis, which is consistent with the fact that chromosomal alignment is terminated during this period (*SI Appendix*, Fig. S3*B*).

These processes would be intrinsically controlled by transcription factors. Therefore, we looked at the expression dynamics in vivo and in vitro of key transcription factors involved in oogenesis. The expression dynamics of *Figla*, *Nobox*, *Sohlh1*, *Sohlh2*, and *Lhx8* were similar between oocytes in vivo and in vitro (Fig. 2*C*). In addition, genes up-regulated in growing oocytes in the activated follicles, such as *Zp1* and *Zp3*, also exhibited similar expression dynamics between oocytes in vivo and in vitro (Fig. 2*C*). In contrast, *Foxo3* had a consistently low expression level in oocytes throughout the IVDi culture (Fig. 2*C*). This low-level expression of the *Foxo3* gene may be one of the reasons that primordial follicles were barely formed in vitro.

**Induction of the Dormant State by Forced Expression of Constitutively Active FOXO3.** To test whether *Foxo3* is sufficient for establishing the dormant state in the culture system, the constitutively active form of FOXO3 (*Foxo3dNES*) (10) was enforcedly expressed by a *c-kit* promoter in the oocytes during IVDi culture (*SI Appendix*, Fig. S4 *A* and *B*). Transcriptional activity of the *c-kit* promoter in IVDi culture was confirmed by using *c-kit–mCherry* reporter construct (*SI Appendix*, Fig. S4*C*). We also confirmed integration of the *Foxo3dNES* transgene by qPCR and maintenance for a pair of X chromosomes by allele-specific PCR (*SI Appendix*, Fig. S4 *D* and *E*). In *Foxo3dNES* transgenic (Tg) ESCs, the total (endogenous and exogenous) *Foxo3* expression was much higher than in the parental ESCs (*SI Appendix*, Fig. S4*F*): The total expression level of *Foxo3* in transgenic oocytes at D21 was more than four times higher than that in wild-type (WT) oocytes and was therefore comparable to that in P3 oocytes in vivo (Fig. 2*C* and *SI Appendix*, Fig. S4*G*). The number of oocytes formed by *Foxo3dNES* Tg ESCs in IVDi was comparable to the number induced from WT ESCs (Fig. 3*A*). Interestingly, the number of small oocytes derived from *Foxo3dNES* Tg ESCs was increased in rOvaries (Fig. 3*B*). As expected, IF analysis confirmed the nuclear localization of FOXO3 in the *Foxo3dNES* Tg oocytes (Fig. 3*C*). SOHLH1, a transcription factor enriched in oocytes in primordial follicles (11), was expressed in the small *Foxo3dNES* Tg oocytes (Fig. 3*D*). Conversely, GDF9, a growth factor enriched in growing oocytes (12), was nearly absent from the small *Foxo3dNES* Tg oocytes (Fig. 3*D*). This expression pattern was similar to that of oocytes in vivo (*SI Appendix*, Fig. S5 *A* and *B*). These data demonstrated that enforced expression of constitutively active FOXO3 led to an induction of the dormant state, to some extent, in IVDi culture.

**Limited Effect of FOXO3 on the Dormant Oocytes In Vitro.** To further investigate the effect of enforced *Foxo3dNES* expression, we performed transcriptome analysis of oocytes in vitro derived from *Foxo3dNES* Tg ESCs and WT ESCs. To rigorously evaluate the effect of *Foxo3dNES* Tg, cDNA libraries were constructed from sorted SC-positive oocytes containing large oocytes. PCA demonstrated that by the expression of *Foxo3dNES* Tg, the transcriptome profile of the oocytes in culture at D21 became closer to that of the dormant oocytes in vivo (P3, P4 small, and P6 small) (Fig. 4*A*). On the other hand, it also suggested that the transcriptomes of *Foxo3dNES* Tg oocytes were still different from those of the dormant oocytes in vivo. This might have been due to the absence of another factor involved in establishing the dormant state.

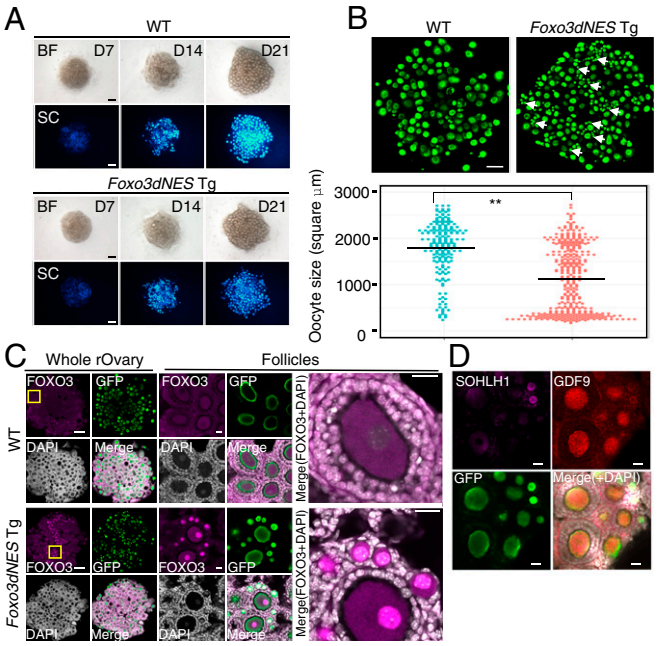


**Fig. 3.** Partial restoration in vitro of small oocytes by enforced expression of *Foxo3*. (*A*) Differentiation of *Foxo3dNES* Tg oocytes during IVDi. Images of rOvaries containing oocytes from the WT or *Foxo3dNES* Tg ESCs are shown. The number at the upper right indicates the days of culture. (Scale bars, 200 μm.) (*B*) *Foxo3dNES* Tg oocytes in rOvaries. Z-stack IF images of GFP (BV and/or SC) (*B*, *Upper*) and oocyte size (area) at D21 (*B*, *Lower*) are shown. Arrows indicate small oocytes in the rOvary. (Scale bar, 200 μm.) The plots were compiled from two independent experiments. Mean values are indicated as lines. $^{**}P < 0.01$ (using Student's *t* test). (*C*) IF analysis of WT and *Foxo3dNES* Tg oocytes at D21. IF images of FOXO3, GFP (BV and/or SC), and DAPI are shown. [Scale bars, 200 μm (whole rOvaries) and 20 μm (follicles).] (*D*) Expression of oocyte markers in *Foxo3dNES* Tg oocytes. IF images of SOHLH1, GFP (BV and/or SC), and GDF9 are shown. (Scale bars, 20 μm.)

To identify such a factor, we compared the transcriptomes of *Foxo3dNES* Tg oocytes and WT ESC-derived oocytes. We identified 176 and 71 genes that were up- and down-regulated in *Foxo3dNES* Tg oocytes compared with oocytes derived from WT ESCs, respectively (Fig. 4*B*). Among the 176 up-regulated genes, 57 had a sequence similar (>90% homology) to FOXO3-binding motif(s) at the putative promoter region 1 kb upstream of the transcription start site (TSS) (*SI Appendix*, Fig. S6). Several of these 57 genes, including *Btg2*, *Cfh*, *Rhob*, *Cyr61*, and *Cav1*, were previously reported to be direct targets of FOXO3. On the other hand, 119 of the 176 up-regulated genes had no FOXO3-binding motif within the 1-kb region upstream of TSS, indicating that a certain number of genes were up-regulated indirectly. Among the 71 down-regulated genes, 22 had a sequence similar to FOXO3-binding motif(s) at the putative promoter region 1 kb upstream of the TSS (*SI Appendix*, Fig.S6). GO analysis showed that the up-regulated genes were related to "response to hypoxia" (Fig. 4*C*), thus indicating a close relationship between FOXO3 and hypoxia. Consistent with such a relationship, the transcriptomes of oocytes in vivo during the transition from embryonic oocytes to the dormant state showed increased expression of genes related to response to oxidative stress and the oxidation-reduction process (*SI Appendix*, Fig. S3*B*). Moreover, several reports have suggested that the function of FOXO3 is relevant to a hypoxic condition (13–15). Based on these findings, we postulated that hypoxia has a positive effect on construction of the dormant state in oocytes.

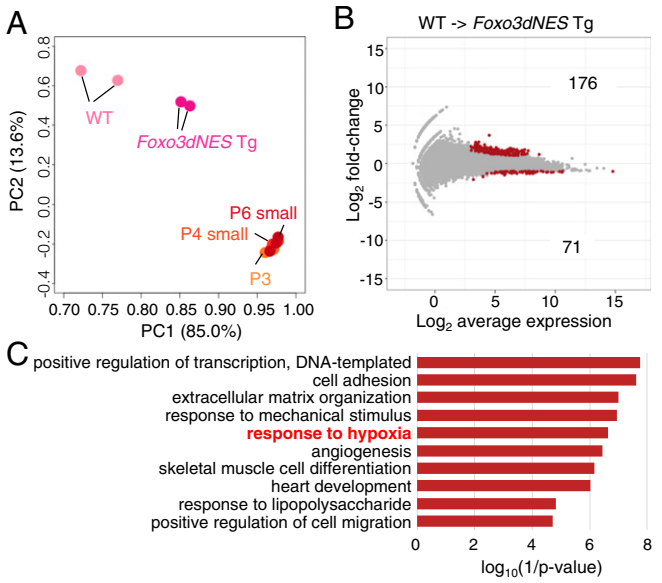


**Fig. 4.** Identification of hypoxia as a possible factor for the dormant state. (*A*) PCA of the WT and *Foxo3dNES* Tg oocytes at D21 in vitro and P3, P4 small, and P6 small oocytes in vivo. (*B*) DEGs between the WT and *Foxo3dNES* Tg oocytes. DEGs were defined by the condition of $Log_2$fold-change >1, $Log_2$averageCPM > 3, and false discovery rate (FDR) < 0.01. The numbers of the DEGs are shown as in the plot. (*C*) GO analysis of the DEGs. GO analysis was performed for the 176 up-regulated genes in *Foxo3dNES* Tg oocytes identified in *B*. The $log_{10}$(1/*P* value) values are shown.

**Hypoxia Is Involved in Establishment of the Dormant Oocytes.** In keeping with our hypothesis, IVDi culture under a 5% $O_2$ condition provided a number of small oocytes in rOvaries (Fig. 5*A*). Quantification analysis confirmed that the low oxygen concentration caused a drastic decrease in the oocyte size (Fig. 5*A*). IF analysis revealed that FOXO3 was localized in the nuclei of the small oocytes (Fig. 5*B*). These small oocytes also showed higher expression of SOHLH1 and lower expression of GDF9 compared with the growing oocytes (Fig. 5*C*). By comparing the transcriptome between *Foxo3dNES* Tg and hypoxia, the dormant state of the oocytes relied more on hypoxia than *Foxo3dNES* Tg (Fig. 5*D*). We next examined the combined effect of hypoxia plus *Foxo3dNES* Tg during IVDi. The size of oocytes under the combined condition was further decreased (Fig. 5 *A* and *E*). The transcriptome data showed that the gene-expression profiles of *Foxo3dNES* Tg oocytes cultured under a hypoxic condition was closer to those of dormant oocytes in vivo than to those of *Foxo3dNES* Tg oocytes under a normoxic condition or oocytes from WT ESCs under a hypoxic condition (Fig. 5 *E* and *D*). To understand the FOXO3 dependency under hypoxia, we produced *Foxo3* KO ESCs harboring a pair of X chromosomes (*SI Appendix*, Fig. S7 *A–C*) and then induced oocytes from the *Foxo3* KO ESCs. The average size of *Foxo3* KO oocytes was comparable to that of WT oocytes under a normoxic condition, and, as expected, there was no fraction of small oocytes among the oocytes derived from *Foxo3* KO ESCs (Fig. 5*A*). In sharp contrast, under the hypoxic condition, the size of *Foxo3* KO oocytes was significantly increased, compared with oocytes from WT ESCs (Fig. 5*A*). IF analysis confirmed the loss of the FOXO3 signal in IVDi using *Foxo3* KO ESCs (Fig. 5*F*). Interestingly, the size of the *Foxo3* KO oocytes under the hypoxic condition was not completely restored to that of the *Foxo3* KO oocytes under the normoxic condition (Fig. 5*A*). These results demonstrated that hypoxia plays a positive role on construction of the dormant state in oocytes and that FOXO3 is one of the effectors downstream of hypoxia.

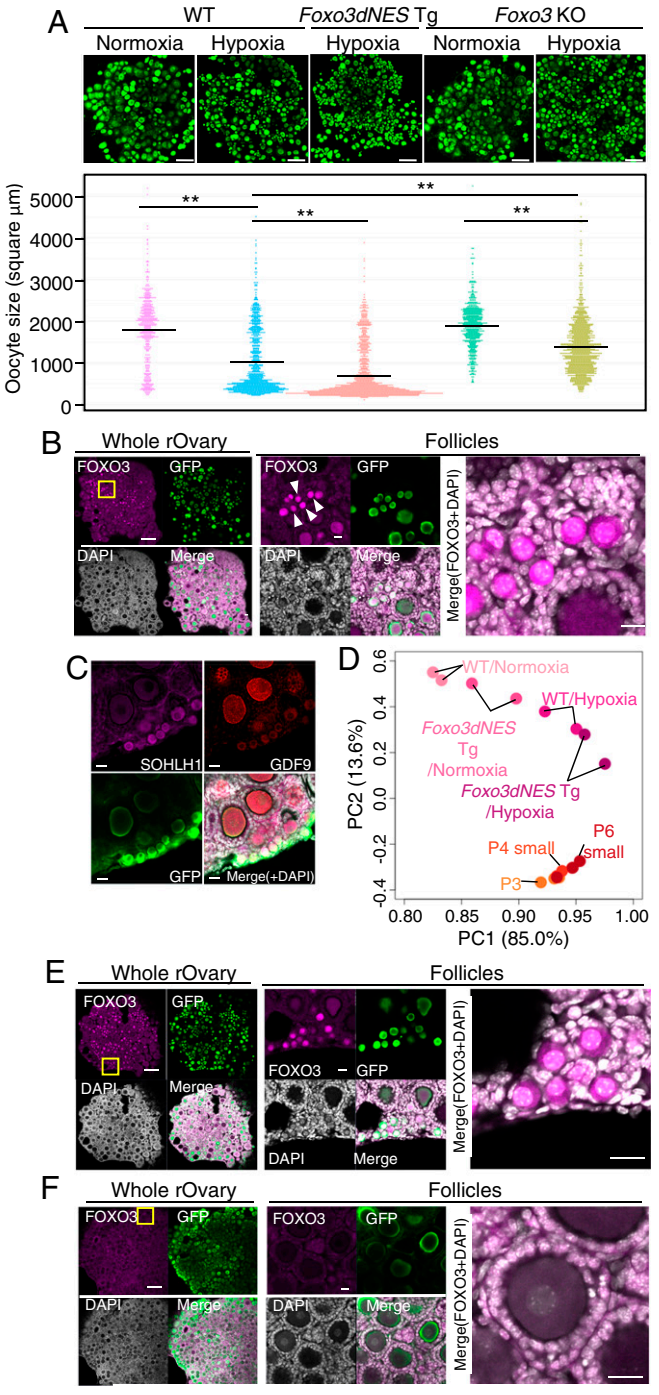


**Fig. 5.** Induction of the dormant state under a hypoxic condition through FOXO3. (*A*) Oocyte size under a hypoxic condition. Z-stack IF images of GFP (BV and/or SC) (*A*, *Upper*) and oocyte size (area) at D21 (*A*, *Lower*) are shown. The plots were compiled from two independent experiments. Mean values are indicated as lines. $^{**}P < 0.01$ (using the Tukey–Kramer method). (*B*) FOXO3 localization under the hypoxic condition. IF images of FOXO3, GFP (BV and/or SC), and DAPI in oocytes at D21 are shown. The yellow box in the Whole rOvary is the area shown in Follicles. [Scale bars, 200 μm (whole rOvary) and 20 μm (Follicles).] (*C*) Expression of oocyte markers under the hypoxic condition. IF images of SOHLH1, GFP (BV and/or SC), and GDF9 are shown. (Scale bars, 20 μm.) (*D*) PCA of oocytes under each condition. (*E* and *F*) Histology and FOXO3 expression. IF images of FOXO3, GFP (BV and/or SC), and DAPI in *Foxo3dNES* Tg (*E*) or Foxo3 KO (*F*) oocytes at D21 under the hypoxic condition are shown. Details are the same as in *B*.

**Hypoxia-Inducible Factor Function in Hypoxic Effect on Establishment of the Dormant State In Vitro.** Given that hypoxia induces several pathways, hypoxia-inducible factors (HIFs) are a strong candidate of a downstream effector. *Hif1a* and *Hif2a* were expressed in oocytes including P3, P4 small oocytes, and P6 small oocytes (*SI Appendix*, Fig. S8*A*). Consistently, HIF1A and HIF2A were detected in the oocytes at D21 of the hypoxic culture (Fig. 6*A*). The addition of YC-1, an inhibitor of both HIF1A and HIF2A (16), to IVDi culture under the hypoxic condition selectively eliminated small oocytes in a dose-dependent manner (Fig. 6*B*). Although the total number of oocytes appeared to decrease, the decrement was almost entirely due to the loss of small oocytes (area < 1,000 $\mu m^2$) (Fig. 6*B* and *SI Appendix*, Fig. S8 *B* and *C*). These results demonstrated that HIF1A and/or HIF2A play a role in sustaining dormant oocytes as a downstream effector of hypoxia.

HIFs are known to change metabolic pathways by promoting anaerobic glycolysis and inhibiting oxidative phosphorylation (OXPHOS). Therefore, we examined the reliance of oocytes on OXPHOS under normoxic and hypoxic conditions. Addition of rotenone, an inhibitor of OXPHOS, to IVDi culture completely abolished oocyte formation under the normoxic condition, whereas a number of oocytes remained under the hypoxic condition (Fig. 6*C* and *SI Appendix*, Fig. S8*D*). Interestingly, small oocytes preferentially remained under the hypoxic condition with rotenone, and the percentage of large oocytes (area > 1,000 $\mu m^2$) was significantly decreased under this condition (*SI Appendix*, Fig. S8*E*). These results suggested that dormant oocytes under a hypoxic condition are less dependent on OXPHOS, compared with growing oocytes. Our findings suggest that hypoxia activates HIFs that endow the small oocytes with an anaerobic metabolic program. Interestingly, it has been reported that FOXO3 antagonizes OXPHOS through repression of a set of nuclear-encoded mitochondrial genes (17). Taking these results together, we conclude that hypoxia orchestrates the dormant state of oocytes through FOXO3 and HIFs.

## Discussion

In the in vitro oocyte differentiation system, most of the oocytes in rOvaries bypassed the dormant state and were activated directly into the secondary follicle stage. This was not due to any suboptimal conditions of the culture system, since such a direct activation of oocyte growth has also been observed in rOvaries (18) and E12.5 ovaries (19) transplanted to adult mice. These findings indicated that a temporal regulation in vivo during the perinatal stage is crucial for establishment of the dormant state in oocytes. Distinct differentiation processes between the in vivo and in vitro oocytes were clearly revealed by comparison of their transcriptomes (Fig. 2*A*). Interestingly, based on their gene-expression profiles in vivo, the dormant oocytes were much more different from growing oocytes (P4 and P6 large) than from embryonic oocytes (E18.5 or earlier). This suggested two possibilities: There is a rapid and dynamic expression change during the exit from the dormant state, and the dormant state is gradually established in the oocytes from late gestation to the neonatal stage. The GO analysis indicated that genes involved in the oxidation-reduction process become active during establishment of the dormant state. Genes up-regulated during this period include *Prdx2*, *Prdx3*, *Prdx5*, *Gpx1*, and *Gpx4*, which regulate antioxidant reaction (*SI Appendix*, Fig. S3*B*). Moreover, the GO term "glutathione metabolic process" is also involved in the antioxidant reaction. These findings suggested that oxidative stress, such as that potentially generated under a hypoxic condition, declines in oocytes during the transition.

Among the key transcription factors for oogenesis, *Foxo3* expression was constantly low in vitro (Fig. 2*C*). Enforced expression of constitutively active FOXO3 partially restored the transcriptome to the dormant state (Fig. 4*A*) and decreased the size of the oocytes (Fig. 3 *B* and *C*). These results are largely consistent with reported genetic studies in vivo, in which enforced FOXO3 expression in mice caused retardation of follicle growth (20, 21). However, in our present experiments, we also found that growing oocytes with a strong nuclear FOXO3 signal were observed (Fig. 3*C*) and that the transcriptome of *Foxo3dNES* Tg oocytes was still far from the dormant state

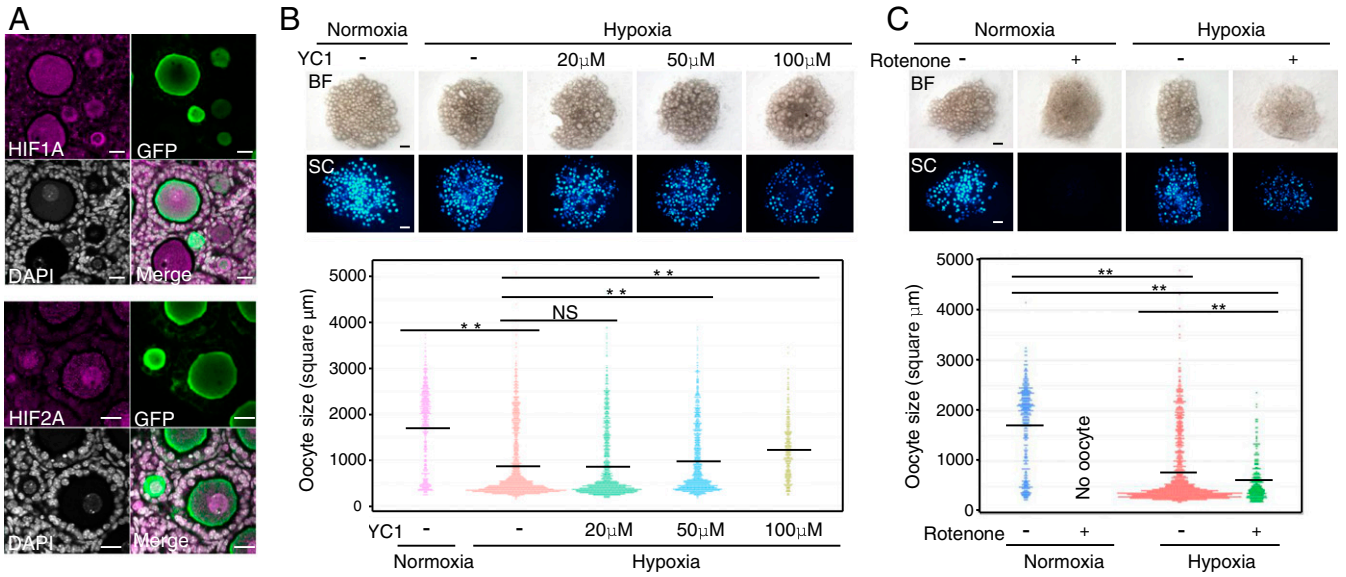


**Fig. 6.** Involvement of HIFs in formation of small oocytes in IVDi culture under a hypoxic condition. (*A*) Expression of HIF proteins. IF images of HIF1A, HIF2A, GFP (BV and/or SC), and DAPI are shown. (Scale bars, 20 μm.) (*B*) Effect of YC-1 on formation of small oocytes. Images of BF and SC in rOvaries at D21 (*B*, *Upper*) and oocyte size (*B*, *Lower*) under the indicated condition are shown. (Scale bars, 200 μm.) The plots were compiled from two independent experiments. Mean values are indicated as lines. $^{**}P < 0.01$ (using Dunnett's test). NS, not significant. (*C*) Effect of OXPHOS inhibition on the formation of small oocytes. Images of BF and SC in rOvaries at D21 (*C*, *Upper*) and oocyte size (*C*, *Lower*) under the indicated condition are shown. (Scale bars, 200 μm.) The plots were compiled from two independent experiments. Mean values are indicated as lines. $^{**}P < 0.01$ (using the Tukey–Kramer method).

in vivo (Fig. 4*A*). These findings suggested an environmental factor that only exists in vivo. This study revealed that one of the environmental factors is hypoxia. Hypoxia induced a large number of small oocytes with nuclear localization of FOXO3 in the IVDi culture system (Fig. 5*A*). The effect was partially, but not completely, diminished by disruption of the *Foxo3* gene (Fig. 5*A*). These findings suggested that the FOXO3 function is only one among numerous functions downstream of hypoxia during the establishment of the dormant state of oocytes. It is noteworthy that, even under the combined condition of hypoxia plus *Foxo3dNES* Tg, the gene-expression profiles in oocytes in culture were not identical to those in oocytes in vivo (Fig. 5*D*). This suggests that one or more other factors are involved in regulating the dormant state. In the future, the identification of any such factors should be pursued by using the present culture system.

In this study, small oocytes in culture were selectively eliminated by the addition of an HIF inhibitor (Fig. 6*B*). HIFs are the master transcriptional regulators involved in oxygen homeostasis, angiogenesis, anaerobic metabolism, tumorigenesis, and inflammation (22). A major role of HIFs is to promote anaerobic glycolysis by transactivating genes encoding glucose transporters and glycolytic enzymes (23, 24). Interestingly, FOXO3 plays a role in decreasing mitochondrial mass and oxygen consumption by repressing a set of nuclear-encoded mitochondrial genes (17). This study demonstrated that small oocytes were more tolerant of rotenone, an inhibitor of OXPHOS, than large oocytes (Fig. 6*C* and *SI Appendix*, Fig. 8 *D* and *E*). These findings suggested that HIFs and FOXO3 have a synergistic effect on a particular metabolic program in dormant oocytes. Hypoxia induces reactive oxygen species (ROS) and thereby subjects the cells to oxidative stress. In the dormant state of oocytes, ROS produced under a hypoxic condition may be attenuated by genes related to response to oxidative stress or the oxidative-reduction process, which are downstream of FOXO3. In support of this notion, it has been reported that protection from oxidative stress is regulated by FOXO3 in colon carcinoma cells (25). It is widely known that HIFs are involved in the reduction of ROS (26, 27). Detoxification of ROS is particularly important in oocytes, as they are the sole cell type to generate the next generation. The dormant state can be established under hypoxia, but at the same time, it must protect the quality of the oocytes against oxidative stress. This double-edged condition is the nature of the dormant state of oocytes in the primordial follicles, which are maintained for a long period of time in the ovary.

## Methods

**IVDi Culture.** IVDi culture was performed as described (7). rOvaries (containing 2,500 PGCLCs and 37,500 gonadal somatic cells or 5,000 PGCLCs and 75,000 gonadal somatic cells) were placed on Transwell-COL membranes and cultured under the normoxic condition (20% $O_2$ and 5% $CO_2$ at 37 °C) or the hypoxic condition (5% $O_2$ and 7% $CO_2$ at 37 °C). For inhibitor experiments, YC-1 (Sigma) was added from D8 to D21, and rotenone (Sigma) was added from D17 to D21 during the IVDi culture. DMSO was used as a vehicle.

**Measurement and Counting of Oocytes.** Green fluorescent protein (GFP) and DAPI images were obtained at depth intervals of 10 μm by using an LSM700 confocal microscope. The largest section of each oocyte was selected, and then the area of the GFP signal from the oocyte was measured and the total number of oocytes was counted by using ImageJ software.

**Establishment of Transgenic ESCs.** For construction of *Foxo3dNES*, the nuclear export signal was disrupted by converting the amino acids (M375A, L377A, L381A, L389A, L390A, I393A, and L395A) (10). The PGK-promoter and puromycin-resistance gene were obtained from the R26pM2rtTA vector (Addgene catalog no. 47381). A 656-bp region of the *c-kit* promoter (28) was amplified from genomic DNA of WT ESCs. All fragments were combined into a PiggyBac vector by using an In-Fusion HD Cloning Kit (TAKARA). pCMV-hyPBase (Wellcome Trust Sanger Institute), PB-ckit promoter-Foxo3dNES, and pEF1-IRES-DsREdexpress2 were transfected into Blimp1–mVenus and Stella–ECFP H18 ESCs by Lipofectamine 2000 (Thermo). After culturing for 24 h, DsRed-positive cells were sorted by a FACS Aria II and cultured with 1 μg/mL puromycin (InvivoGen). At 6 d of culture, single colonies were picked up and seeded on mouse embryonic fibroblasts.

**ACKNOWLEDGMENTS.** We thank Y. Ohkwawa for technical assistance with the RNA-seq analysis; K. Kitajima and C. Meno for providing microscopes; K. Nakajima for providing the PB vector; F. Arai for providing the FACS Aria II; S. Lopes for proofreading; and M. Saitou for providing BVSC mice. We also thank the Research Support Center, Research Center for Human Disease Modeling, Kyushu University Graduate School of Medical Sciences for technical assistance. This study was supported in part by Ministry of Education, Culture, Sports, Science, and Technology KAKENHI Grants-in-Aid 17H01395, 18H05544, and 18H05545 (to K.H.) and 18K06261 (to G.N.); Management Expenses Grants of Kyushu University (K.H.); Advanced Computational Scientific Program of Research Institute for Information Technology, Kyushu University; the Uehara Memorial Foundation (K.H.); the Takeda Science Foundation (K.H.); a Hayashi Grant-in-Aid for Basic Medical Research (Kyushu University) (K.H.); and a Japan Society for the Promotion of Science Research Fellowship (N. Hamazaki and S.S.).

1. M. E. Pepling, A. C. Spradling, Female mouse germ cells form synchronously dividing cysts. *Development* **125**, 3323–3328 (1998).
2. A. McLaren, Germ and somatic cell lineages in the developing gonad. *Mol. Cell. Endocrinol.* **163**, 3–9 (2000).
3. M. E. Pepling, A. C. Spradling, Mouse ovarian germ cell cysts undergo programmed breakdown to form primordial follicles. *Dev. Biol.* **234**, 339–351 (2001).
4. D. H. Castrillon, L. Miao, R. Kollipara, J. W. Horner, R. A. DePinho, Suppression of ovarian follicle activation in mice by the transcription factor Foxo3a. *Science* **301**, 215–218 (2003).
5. P. Reddy *et al*., Oocyte-specific deletion of Pten causes premature activation of the primordial follicle pool. *Science* **319**, 611–613 (2008).
6. O. Hikabe *et al*., Reconstitution in vitro of the entire cycle of the mouse female germ line. *Nature* **539**, 299–303 (2016).
7. K. Hayashi, O. Hikabe, Y. Obata, Y. Hirao, Reconstitution of mouse oogenesis in a dish from pluripotent stem cells. *Nat. Protoc.* **12**, 1733–1744 (2017).
8. Y. Ohinata, M. Sano, M. Shigeta, K. Yamanaka, M. Saitou, A comprehensive, non-invasive visualization of primordial germ cell development in mice by the Prdm1-mVenus and Dppa3-ECFP double transgenic reporter. *Reproduction* **136**, 503–514 (2008).
9. K. Hayashi, H. Ohta, K. Kurimoto, S. Aramaki, M. Saitou, Reconstitution of the mouse germ cell specification pathway in culture by pluripotent stem cells. *Cell* **146**, 519–532 (2011).
10. A. Brunet *et al*., 14-3-3 transits to the nucleus and participates in dynamic nucleocytoplasmic transport. *J. Cell Biol.* **156**, 817–828 (2002).
11. S. A. Pangas *et al*., Oogenesis requires germ cell-specific transcriptional regulators Sohlh1 and Lhx8. *Proc. Natl. Acad. Sci. U.S.A.* **103**, 8090–8095 (2006).
12. S. A. McGrath, A. F. Esquela, S. J. Lee, Oocyte-specific expression of growth/differentiation factor-9. *Mol. Endocrinol.* **9**, 131–136 (1995).
13. W. J. Bakker, I. S. Harris, T. W. Mak, FOXO3a is activated in response to hypoxic stress and inhibits HIF1-induced apoptosis via regulation of CITED2. *Mol. Cell* **28**, 941–953 (2007).
14. X. Liu *et al*., Forkhead transcription factor 3a (FOXO3a) modulates hypoxia signaling via upregulation of the von Hippel-Lindau gene (VHL). *J. Biol. Chem.* **291**, 25692–25705 (2016).
15. S. Zhang *et al*., FoxO3a modulates hypoxia stress induced oxidative stress and apoptosis in cardiac microvascular endothelial cells. *PLoS One* **8**, e80342 (2013).
16. S. H. Li *et al*., A novel mode of action of YC-1 in HIF inhibition: Stimulation of FIH-dependent p300 dissociation from HIF-1α. *Mol. Cancer Ther.* **7**, 3729–3738 (2008).
17. K. S. Jensen *et al*., FoxO3A promotes metabolic adaptation to hypoxia by antagonizing Myc function. *EMBO J.* **30**, 4554–4570 (2011).
18. K. Hayashi *et al*., Offspring from oocytes derived from in vitro primordial germ cell-like cells in mice. *Science* **338**, 971–975 (2012).
19. S. Matoba, A. Ogura, Generation of functional oocytes and spermatids from fetal primordial germ cells after ectopic transplantation in adult mice. *Biol. Reprod.* **84**, 631–638 (2011).
20. L. Liu *et al*., Infertility caused by retardation of follicular development in mice with oocyte-specific expression of Foxo3a. *Development* **134**, 199–209 (2007).
21. E. Pelosi *et al*., Constitutively active Foxo3 in oocytes preserves ovarian reserve in mice. *Nat. Commun.* **4**, 1843 (2013).
22. H. Choudhry, A. L. Harris, Advances in hypoxia-inducible factor biology. *Cell Metab.* **27**, 281–298 (2018).
23. I. Papandreou, R. A. Cairns, L. Fontana, A. L. Lim, N. C. Denko, HIF-1 mediates adaptation to hypoxia by actively downregulating mitochondrial oxygen consumption. *Cell Metab.* **3**, 187–197 (2006).
24. G. L. Wang, B. H. Jiang, E. A. Rue, G. L. Semenza, Hypoxia-inducible factor 1 is a basic-helix-loop-helix-PAS heterodimer regulated by cellular O2 tension. *Proc. Natl. Acad. Sci. U.S.A.* **92**, 5510–5514 (1995).
25. G. J. P. L. Kops *et al*., Forkhead transcription factor FOXO3a protects quiescent cells from oxidative stress. *Nature* **419**, 316–321 (2002).
26. S. Stegen *et al*., HIF-1α promotes glutamine-mediated redox homeostasis and glycogen-dependent bioenergetics to support postimplantation bone cell survival. *Cell Metab.* **23**, 265–279 (2016).
27. T. Zhao *et al*., HIF-1-mediated metabolic reprogramming reduces ROS levels and facilitates the metastatic colonization of cancers in lungs. *Sci. Rep.* **4**, 3793 (2014).
28. T. Tsujimura *et al*., Involvement of transcription factor encoded by the mi locus in the expression of c-kit receptor tyrosine kinase in cultured mast cells of mice. *Blood* **88**, 1225–1233 (1996).